MECHANICAL AND ELECTRICAL PROPERTIES OF CAST Al–Er–Zr ALLOY

[1]Michal LEIBNER, [1]Martin VLACH, [1]Veronika KODETOVÁ, [1]Jozef VESELÝ, [1]Hana KUDRNOVÁ, [1]Miroslav CIESLAR, [1]Sebastien ZIKMUND, [2]Vladivoj OČENÁŠEK, [1,3]František LUKÁČ, [4]Vladimír MÁRA

[1]Charles University, Faculty of Mathematics and Physics, Prague, Czech Republic, EU, mleibner@seznam.cz

[2]SVÚM a.s., Čelákovice, Czech Republic, EU

[3]Academy of Sciences of the Czech Republic, Institute of Plasma Physics, Prague, Czech Republic, EU

[4]Czech Technical University in Prague, Faculty of Mechanical Engineering, Prague, Czech Republic, EU

https://doi.org/10.37904/metal.2021.4222

Abstract

Mechanical and electrical properties of an Al–Er–Zr alloy were investigated. Microhardness and resistometry measurements were supplemented by transmission electron microscopy and scanning electron microscopy. Resistivity decreases during isochronal annealing take place within the following temperature intervals: 150–270 °C, 300–420 °C and 450–570 °C. The isochronal microhardness curve reflects hardening effects at corresponding temperatures. However, no thermal effect was observed in the DSC curves ranging from 25 °C to 600 °C. A transmission electron microscopy observation of the alloy studied isochronally annealed up to 390° C revealed a high density of $L1_2$-structured particles, some of which had nucleated on dislocations. The distinct electrical resistivity, as well as microhardness, changes are in all cases connected with the precipitation and evolution of the Al_3Er, Al_3Zr and/or $Al_3(Er,Zr)$ particles.

Keywords: Precipitation hardening, Al–Er–Zr alloy, resistivity, TEM

1. INTRODUCTION

An addition of Sc to Al alloys increases drastically the strength of an Al alloy due to the formation of a high number density of $L1_2$-structured Al_3Sc precipitates coherent with the aluminum matrix [1, 2]. Further addition of a trace amount of Zr leads to formation of ternary $L1_2$-$Al_3(Sc,Zr)$ precipitates. These ternary particles have both thermodynamic and kinetic tendencies to form a core-shell structure [3-6]. The resulting Zr-rich shell can retard the fast diffusing Sc and therefore impede the coarsening of the precipitates [3, 5, 7].

However, the applications of Sc are restricted due to its high cost. Similarly to Sc, the heavy rare-earth element Er exhibits an Al–Al_3Er eutectic reaction. Al_3Er also exhibits a stable $L1_2$ structure [8]. Er has a larger diffusivity than Sc [9, 10], and thus Al_3Er precipitates nucleate and grow at low temperatures and therefore Al–Er alloys suffer from an early loss of strength [11]. The high matrix/precipitate interfacial energy in case of Al_3Er [12] also indicates low coarsening resistance. Fortunately, it was confirmed that the co-alloying of Er and Zr in Al leads to the precipitation of $L1_2$-phase $Al_3(Er,Zr)$ particles. Li et al. [13] reported the core-shelled structure of $Al_3(Er,Zr)$ in a peak-aged Al–Er–Zr alloy. Just like in case of $Al_3(Sc,Zr)$, the shell rich in Zr can act as diffusional barrier enhancing the coarsening resistance of the precipitates [13].

Despite these findings, the Al–Er–Zr system has not been thoroughly studied and the description of non-homogenised cast Al–Er–Zr alloys is missing. This article reports on the evolution of mechanical and electrical properties of a cast Al–Er–Zr alloy during isochronal annealing.

2. EXPERIMENTAL PROCEDURES

A ternary as-cast alloy with nominal composition of Al–0.25 Er–0.15 Zr (wt%) was studied. The samples were isochronally annealed from room temperature (RT) up to 570 °C in steps of 30 °C/30 min. Heat treatment was performed in a stirred silicone oil bath up to 240 °C (these steps were followed by quenching into liquid nitrogen) and in a furnace with an argon protective atmosphere above 240 °C (followed by quenching into water at RT).

The response of Vickers microhardness (HV0.3) to isochronal annealing was investigated by Wolpert Wilson Micro Vickers 401MVD at ~ 10 °C.

Relative resistivity changes during the isochronal annealing were measured by DC four-point method with a dummy specimen in series at 77 K in liquid nitrogen bath.

Differential scanning calorimetry (DSC) was performed at heating rates of 5, 10 and 20 °C/min in Netzsch DSC 204 Phoenix apparatus. A specimen of mass ~10 mg was placed in Al_2O_3 crucibles. Nitrogen flowed at the rate of 40 ml/min as a protective atmosphere.

The microstructural development was investigated by scanning electron microscopy (SEM) and transmission electron microscopy (TEM) using TESCAN MIRA I LMH, equipped with an X-ray BRUKER microanalyser for energy-dispersive spectroscopy (EDS) measurements, and JEOL 2200FS, respectively. TEM foils were cut from the aged specimens, ground to about 100 μm and then electropolished with an electrolyte solution consisting of 30% nitric acid and 70% methanol at −25 °C.

3. RESULTS AND DISCUSSION

Figure 1 displays the response of the microhardness HV0.3 and relative resistivity changes of the Al–0.25 Er–0.15 Zr alloy to step-by-step isochronal annealing. The initial absolute value of resistivity was determined as 5.06±0.08 nΩ•m. Three distinct decreases of resistivity can be seen in the annealing curve. These occur within the following temperature intervals: 150–270 °C, 300–420 °C and 450–570 °C, the last decrease being the sharpest. The microhardness increases slightly during the first drop of resistivity and peaks at 360 °C (during the second one). The microhardness then drops at 420 °C before peaking again at 480 °C after which it reaches a plateau.

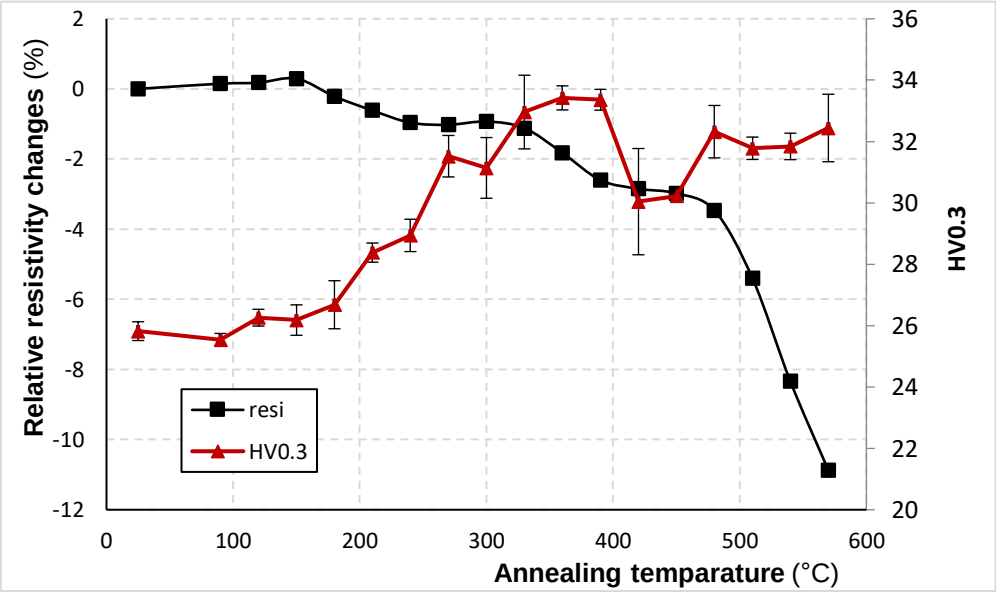

Figure 1 Isochronal annealing curves of resistivity and microhardness

The DSC measurements in heating rates of 5, 10 and 20 °C/min were done in the alloys in addition to resistivity and microhardness measurements. However, no thermal effect was observed in the DSC curves ranging from 25 °C to 600 °C.

SEM micrograph of the alloy in the as-cast state (**Figure 2**) shows a high number density of Er-rich primary precipitates, as analyzed by EDS, indicating that the Er supersaturation in the Al matrix might be relatively low. The eutectic is enriched in Er only as Al–Zr alloys undergo a peritectic transformation [14]. Only small density of dislocations in grain interiors in the as-state of the alloy was observed by TEM. Considering that the number of grain boundaries (millimetre-size grains, roughly estimated from SEM observations) is also very low and do not change significantly during the aging process, the dominating contributing factor to the evolution of electrical resistivity is the change of solute concentrations in the matrix.

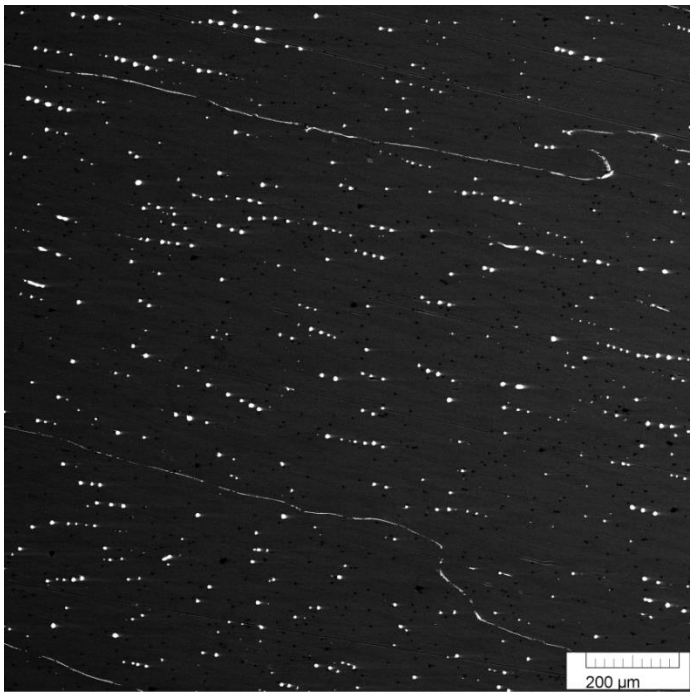

Figure 2 SEM micrograph of the as-cast microstructure

In the available literature focusing on Al–Er–Zr ternary and Al–Er–Sc–Zr quaternary systems, Er is generally believed to precipitate first [12, 13, 15-18], owing to its high diffusivity [10], despite its high critical nucleation radius and critical work of nucleation [12]. The sluggishly diffusing Zr was reported to first precipitate above 400 °C even at lower effective heating rates of isochronal annealing [15, 16]. Therefore, the second microhardness peak and the resistivity changes above 450 °C can be ascribed to Zr.

Figure 3 shows dark-field TEM micrograph of the alloy isochronally annealed up to 390 °C taken with an $L1_2$ superlattice reflection. Based on the above, the displayed particles are most probably Al_3Er. The diffraction pattern shown in **Figure 4** confirms the $L1_2$ structure of the precipitates. The arrows in **Figure 3** point at arrays of heterogeneously precipitated particles. Such arrayed precipitation was also observed in an Al–Sc alloy [19] and Al–Sc–Ti alloy [20] aged at small supersaturation. Low supersaturation means low thermodynamic driving force for nucleation and the precipitates nucleate predominately heterogeneously on dislocations to form an array [20]. The Er supersaturation in the present alloy has probably been considerably lowered by formation of the primary particles (see **Figure 2**). Moreover, the matrix/precipitate interfacial energy is higher for Al_3Er (compared to Al_3Sc) [12] and so its precipitation can be expected to be even more affected by presence of preferential nucleation sites.

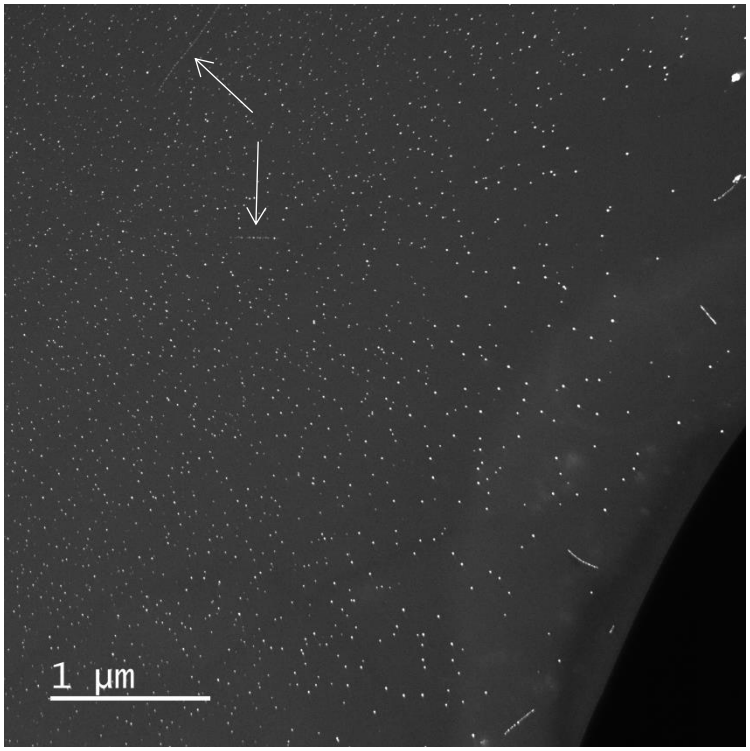

Figure 3 Dark-field TEM image of the alloy isochronally annealed up to 390 °C

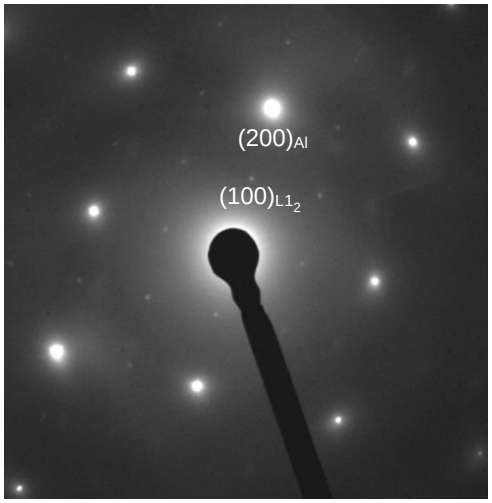

Figure 4 Selected area diffraction pattern of the alloy isochronally annealed up to 390 °C with weak $L1_2$ reflections, beam parallel to $[001]_{Al}$ projection

So far, little effort has been made to describe the early stages of evolution of Al_3Er particles. Vlach et al. [21] investigated phase transformations in an Al–0.2 Sc–0.15 Zr alloy during isochronal annealing and found that prior to Al_3Sc precipitation there was a slight decrease and increase in resistivity and microhardness, respectively. The suggested explanation – Sc clustering – was later proved by positron annihilation spectroscopy [22]. Analogically it can be proposed that the slight resistivity and microhardness changes between 150 °C and 270 °C (see **Figure 1**) are connected to clustering of Er. This statement, however, stems from the analogy to the similar Al–Sc system and is to be proved. Subsequently Al_3Er are formed, resulting in drop of resistivity and peak hardness at about 360 °C. The decline of microhardness at 420 °C is probably

caused by coarsening of the Al_3Er particles. Their dissolution would be accompanied by an increase of resistivity which was not observed.

Nieet al.[15] have reported that the number density of precipitates of Al–Er–Zr alloy is higher than that of Al–Er alloy and there are core–shell Al_3(Er, Zr) precipitates in the Al–Er–Zr alloy with core enriched in Er and shell enriched in Zr. First-principles calculations showed that this core-shell structure is the most stable among all possible precipitation structures in Al–Er–Zr and thus shall account for majority of precipitates [12]. At temperatures greater than 420 °C, the diffusivity of Zr becomes sufficiently large to permit significant diffusion and precipitation of this solute element on previously formed Al_3Er precipitates, causing the second microhardness peak and subsequent microhardness plateau.

4. CONCLUSIONS

The properties of cast Al–Er–Zr alloy were investigated utilizing microhardness, electrical resistivity measurements, differential scanning calorimetry and observations by electron microscopy. Based on the obtained results, following conclusions can be made:

- The slight resistivity and microhardness changes between 150 °C and 270 °C might stem from clustering of Er.
- The precipitation of Al_3Er particles results in a pronounced hardening effect. Some of these particles nucleated on dislocations.
- No thermal effect was observed in the DSC curves ranging from 25 °C to 600 °C.
- Above 420 °C, Zr most likely precipitates on previously formed Al_3Er nuclei, probably forming a Zr-rich shell.
- In order to describe the decomposition sequence of the Al–Er–Zr system thoroughly, further investigations are required.

ACKNOWLEDGEMENTS

The study was supported by the Charles University, project GA UK No. 103-010/251591.
ML acknowledges support by the project SVV-260582 (Specific Academic Research Projects, Charles University).

REFERENCES

[1] TOROPOVA, L.S., ESKIN, D.G., KHARAKTEROVA, M.L., DOBATKINA, T.V. *Advanced aluminum alloys containing scandium – structure and properties*. Amsterdam: Gordon and Breach Science Publisher, 1998. ISBN 90-5699-089-6.

[2] MICHNA, Š., LUKÁČ, I., OČENÁŠEK, V., KOŘENÝ, R., DRÁPALA, J., SCHNEIDER, H., MIŠKUFOVÁ, A. et al. Aluminium Materials and Technologies from A to Z. Slovakia, Adin s.r.o, Prešov, 2007. ISBN 80-89041-4 *Encyklopedie hliníku*. Prešov: Adin s.r.o., 2005. ISBN 978-80-89244-18-8.

[3] FULLER. C.B., SEIDMAN, D.N., DUNAND, D.C. Mechanical properties of Al(Sc,Zr) alloys at ambient and elevated temperatures. *Acta Materialia*. [online]. 2003, vol. 51, pp. 4803-4814. ISSN 1359-6454. Available from: https://doi.org/10.1016/S1359-6454(03)00320-3.

[4] KOLÁŘ, M., OČENÁŠEK, V., UHLÍŘ, J., STULÍKOVÁ, I., SMOLA, B., VLACH, M., NEUBERT, V. SPERLINK, K. Effect of Sc and Zr additions on microstructure and mechanical properties of conventional cast and P/M aluminium. *Materials Science Forum*. [online]. 2008. vol. 567-568, pp. 357–360. Available from: https://doi.org/10.4028/www.scientific.net/MSF.567-568.357.

[5] KNIPLING, K.E., SEIDMAN, D.N., DUNAND, D.C. Ambient- and high-temperature mechanical properties of isochronally aged Al–0.06Sc, Al–0.06Zr and Al–0.06Sc–0.06Zr (at%) alloys. *Acta Materialia*. [online]. 2011, vol. 59, pp. 943-954. ISSN 1359-6454. Available from: https://doi.org/10.1016/j.actamat.2010.10.017.

[6] VLACH, M., KODETOVÁ, V., ČÍŽEK, J., LEIBNER, M., KEKULE, T., LUKÁČ, F., CIESLAR, M., BAJTOŠOVÁ, L., KUDRNOVÁ, H., ŠÍMA, V., ZIKMUND, S., ČERNOŠKOVÁ, E., KUTÁLEK, P., NEUBERT, V.D., NEUBERT, V. Role of small addition of Sc and Zr in clustering and precipitation phenomena induced in AA7075. *Metals*. [online]. 2021, vol. 11, no. 8. Available from: https://doi.org/10.3390/met11010008.

[7] KNIPLING, K.E., KARNESKY, R.A., LEE, C.P., DUNAND, D.C., SEIDMAN, D.N. Precipitation evolution in Al–0.1Sc, Al–0.1Zr and Al–0.1Sc–0.1Zr (at%) alloys during isochronal aging. *Acta Materialia*. [online]. 2010, vol. 58, pp. 5184-5195. ISSN 1359-6454. Available from: https://doi.org/10.1016/j.actamat.2010.05.054.

[8] ZHANG, Y., GAO, K., WEN, S., HUANG, H., NIE, Z., ZHOU, D. The study on the coarsening process and precipitation strengthening of Al3Er precipitate in Al–Er binary alloy. *Journal of Alloys and Compounds*. [online]. 2014, vol. 610, pp. 27-34. ISSN 0925-8388. Available from: https://doi.org/10.1016/j.jallcom.2014.04.093.

[9] KNIPLING, K.E., DUNAND, D.C., SEIDMAN, D.N. Criteria for developing castable, creep-resistant aluminum-based alloys - A review. *Zeitschrift für Metallkunde/Materials Research and Advanced Techniques*. [online]. 2006, vol. 97, pp. 246-265. Available from: https://doi.org/10.3139/146.101249.

[10] VAN DALEN, M.E., KARNESKY, R.A., CABOTAJE, J.R., DUNAND, D.C., SEIDMAN, D.N. Erbium and ytterbium solubilities and diffusivities in aluminum as determined by nanoscale characterization of precipitates. *Acta Materialia.* [online]. 2009, vol. 57, pp. 4081-4089. Available from: https://doi.org/10.1016/j.actamat.2009.05.007.

[11] ZHANG, Y., GAO, K., WEN, S., HUANG, H., NIE, Z., ZHOU, D. The study on the coarsening process and precipitation strengthening of Al3Er precipitate in Al–Er binary alloy. *Journal of Alloys and Compounds*. [online]. 2014, vol. 610, pp. 27-34. Available from: https://doi.org/10.1016/j.jallcom.2014.04.093.

[12] ZHANG, C., YIN, D., JIANG, Y., WANG, Y. Precipitation of L12-phase nano-particles in dilute Al-Er-Zr alloys from the first-principles. *Computational Materials Science*. [online]. 2019, vol. 162, pp. 171-177. ISSN 0927-0256. Available from: https://doi.org/10.1016/j.commatsci.2019.03.001.

[13] HONGYING, L., JIE, B., JIAOJIAO, L., ZHAOHE, G., XIAOCHAO, L. Precipitation evolution and coarsening resistance at 400°C of Al microalloyed with Zr and Er. *Scripta Materialia.* [online]. 2012, vol. 67, pp. 73-76. ISSN 1359-6462. Available from: https://doi.org/10.1016/j.scriptamat.2012.03.026.

[14] FISCHER, E., COLINET, C. An updated thermodynamic modeling of the Al-Zr system. *Journal of Phase Equilibria and Diffusion*. [online]. 2015, vol. 36, pp. 404-413. Available from: https://doi.org/10.1007/s11669-015-0398-y.

[15] WEN, S.P., GAO, K.Y., LI, Y., HUANG, H., NIE, Z.R. Synergetic effect of Er and Zr on the precipitation hardening of Al–Er–Zr alloy. *Scripta Materialia*. [online]. 2011, vol. 65, pp. 592-595. ISSN 1359-6462. Available from: https://doi.org/10.1016/j.scriptamat.2011.06.033.

[16] BOOTH-MORRISON, C., DUNAND, D.C., SEIDMAN, D. N. Coarsening resistance at 400 °C of precipitation-strengthened Al–Zr–Sc–Er alloys. *Acta Materialia*. [online]. 2011, vol. 59, pp. 7029-7042. ISSN 1359-6454. Available from: https://doi.org/10.1016/j.actamat.2011.07.057.

[17] DE LUCA, A., DUNAND, D.C., SEIDMAN, D.N. Mechanical properties and optimization of the aging of a dilute Al-Sc-Er-Zr-Si alloy with a high Zr/Sc ratio. *Acta Materialia*. [online]. 2016, vol. 119, pp. 35-42, ISSN 1359-6454. Available from: https://doi.org/10.1016/j.actamat.2016.08.018.

[18] VO, N.Q., DUNAND, D.C., SEIDMAN, D.N. Improving aging and creep resistance in a dilute Al–Sc alloy by microalloying with Si, Zr and Er. *Acta Materialia*. [online]. 2014, vol. 63, pp. 73-85. ISSN 1359-6454. Available from: https://doi.org/10.1016/j.actamat.2013.10.008.

[19] MARQUIS, E.A., SEIDMAN, D.N. Nanoscale structural evolution of Al_3Sc precipitates in Al(Sc) alloys. *Acta Materialia*. [online]. 2001, vol. 49, pp. 1909-1919, ISSN 1359-6454. Available from: https://doi.org/10.1016/S1359-6454(01)00116-1.

[20] VAN DALEN, M.E., DUNAND, D.C., SEIDMAN, D.N. Effects of Ti additions on the nanostructure and creep properties of precipitation-strengthened Al–Sc alloys. *Acta Materialia*. [online]. 2005, vol. 53, pp. 4225-4235. ISSN 1359-6454. Available from: https://doi.org/10.1016/j.actamat.2005.05.022.

[21] VLACH, M., STULÍKOVÁ, I., SMOLA, B., ŽALUDOVÁ, N., ČERNÁ, J. Phase transformations in isochronally annealed mould-cast and cold-rolled Al–Sc–Zr-based alloy. *Journal of Alloys and Compounds*. [online]. 2010, vol. 492, pp. 143-148. ISSN 0925-8388. Available from: https://doi.org/10.1016/j.jallcom.2009.11.126.

[22] VLACH, M., ČÍŽEK, J., SMOLA, B., STULÍKOVÁ, I., HRUŠKA, P., KODETOVÁ, V., DANIŠ, S., TANPRAYOON, D., NEUBERT, V. Influence of dislocations on precipitation processes in hot-extruded Al–Mn–Sc–Zr alloy. *International Journal of Materials Research*. [online]. 2018, vol. 109, pp. 583-592. Available from: https://doi.org/10.3139/146.111654.